Utilization of reluctance type mixed pole machine as a tachogenerator

Ragi A. Hamdy
Electrical Engg. Dept., Faculty of Engg., Alexandria University, Alexandria, Egypt
e-mail: ragihamdy@hotmail.com

This paper presents a novel tachogenerator as a new application for the mixed pole machine where two stator windings with different number of poles are used. A prototype is developed for system verification. The winding function theory is used for the calculation of machine winding inductances. Performance assessment is based on both a finite element model and experimental results from the developed prototype. The proposed tachogenerator is brushless with low inertia simple construction and linear voltage-speed relationship over a wide speed range.

يقدم هذا البحث نوع مبتكر من مولدات التاكو كتطبيق جديد للآلات ذات الأقطاب المختلطة والتى يكون فيها اثنين من اللفائف فى العضو الثابت لكل منهما عدد مختلف من الأقطاب. تم بناء نموذج عملى لاثبات عمل النظام المقترح كما تستخدم نظرية دالة اللفائف لحساب محاثة اللفائف. ولقد تم تقييم الأداء بناء على كل من نتائج التمثيل باستخدام تحليل العناصر المحدودة والنتائج العملية. ومولد التاكو المقترح ليس له فرش قليل القصور الذاتى وبسيط التصميم وله علاقة خطية للجهد مع السرعة على مدى واسع للسرعة.

Keywords: Tachogenerators, Mixed pole machine, Winding function, Finite element

1. Introduction

Tachogenerators are used in speed control applications and servo systems to provide a voltage signal which is proportional to rotational speed. This voltage is applied to the tachometer to measure the machine speed or may be used as a feedback signal that may be compared with a reference value that corresponds to the required machine speed.

Traditionally, tachogenerators have been purpose-designed generators. They are different from the conventional power generator, since they should provide some special features to operate as tachogenerators. Low inertia of the tachogenerator rotating parts is essential to avoid affecting the mechanical power and torque of the controlled machine. The electrical time constant of the windings should be small to minimize its effect on the controlled motor transient response. It is also crucial for the tachogenerator to have a linear relationship between the speed and the generated voltage over the operating speed range.

One of the commonly used tachogenerators is the dc tachogenerator, which is a purpose-designed dc generator with alnico permanent magnets, skewed armatures, multi-segment commutators and silver leaded brushes [1]. This type suffers from voltage ripples at low speeds due to commutation action. Also, it requires maintenance due to commutator. This makes this type more expensive. However, the main advantage of this type is its linear speed voltage relationship.

The widespread application of brushless motors in servosystems has led to a demand for brushless tachogenerators. This gives way to the AC tachogenerator [2]. This type gives an AC voltage proportional to the speed. The frequency of this voltage is constant and independent of machine speed. It can be considered as a two phase induction machine. One of the stator phases is connected to a constant voltage, constant frequency supply. This voltage is called the field voltage. The voltage induced across the other phase is proportional to the speed. The voltage speed relationship is linear for low speeds. As the speed increases the relationship becomes nonlinear. However the main advantage of this type is its simple construction and absence of brushes which minimize its maintenance requirements.

Mixed Pole Machines (MPM) or Brushless Doubly Fed Machines (BDFM) are self cascaded dual stator machines [3 – 6]. MPM comprises two stator windings with different number of pole pairs and a specially designed rotor. There are three rotor configurations; namely nested cage, reluctance, and reluctance wound [7 – 12]. MPM has various potential applications in low-cost adjustable speed drives and variable speed generators such as wind energy schemes [13 - 17], electric vehicles [18], and it can be used in applications that require control of both rotor torque and rotor electrical power, such as contactless rotational antennas and turret systems [19]. This paper proposes a novel tachogenerator as an application for mixed pole machines. The main advantage of this new type is its linear voltage speed relationship over a wide speed range, low inertia, simple construction, and absence of brushes. The transient model of the proposed tachogenerator and the voltage speed relationship are investigated for DC and AC excitations. A Finite Element Analysis (FEA) model is developed to investigate the flux distribution, the generated voltage waveform, and calculate the generated voltage–speed relationship.

2. Construction

The stator of an existing squirrel cage induction machine is used to construct the prototype of the proposed tachogenerator. The 24 slot stator is rewound to host two stator windings. First winding (excitation winding) is a 2-pole three phase winding. This winding produces the machine magnetic field. The other stator winding (auxiliary winding) is a single phase 4-pole winding. The voltage induced in this winding is proportional to the machine speed. This voltage is then applied to a peak detector that is composed of a diode in series with a capacitor to obtain a DC voltage proportional to the rotating speed. The rotor is a reluctance rotor with three saliencies, as shown in fig. 1. The rotor is made by cutting every other three slots of the existing 18 slot, squirrel cage rotor. The short circuit rings of the rotor winding are removed so as to remove the effect of the rotor windings. However this will still affect the rotor effective pole arc.

3. Determination of machine Inductances

Fig. 1 shows the machine model of the proposed tachogenerator with both four-pole and two-pole windings. It is assumed that the number of turns for the 4-pole auxiliary windings is N_1 and that of the 2-pole excitation winding is N_2.

Calculation of machine inductances can be calculated by a variety of means including field theory, finite elements and various circuit approaches. A particular convenient approach is the winding functions in which the inductances of the machine are calculated by the integral expression representing the placement of winding turns along the air gap periphery [20-21]. The method is particularly convenient for the analysis of unusual machines since it assumes no symmetry in the placement of any motor coil in the slots. As in most inductance calculations it is assumed that the iron of the rotor and stator has infinite permeability and saturation is neglected. Also, the stator surface is considered smooth and the effects of slots can be corrected by modifying air gap length by carter coefficient.

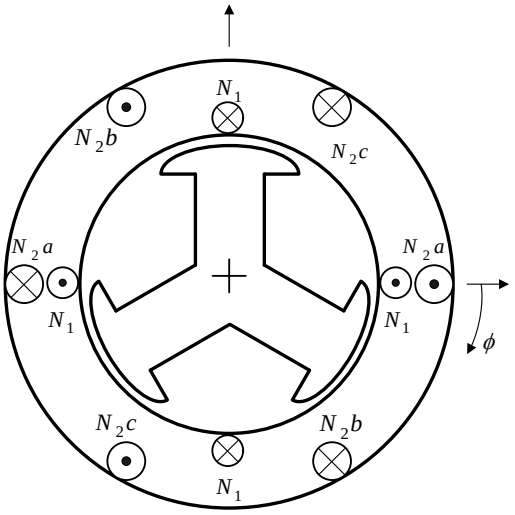

Fig. 1. 4/2 poles MPM with reluctance rotor.

For the sake of simplicity, the analysis for the considered machine is based on sinusoidal

distribution of the stator excitation windings. The stator harmonics are assumed negligible.

According to winding function theory, the mutual inductance between any two windings *i* and *j* in any electric machine can be computed by the following eq. [12]:

$$L_{ij}(\theta_m) = \mu_o.R.l\int_0^{2\pi} g^{-1}(\theta_m,\varphi).N_i(\theta_m,\varphi).N_j(\theta_m,\varphi).d\varphi\,, \tag{1}$$

Where,

μ_o	space permeability,
R	rotor radius,
l	rotor length,
θ_m	the rotor angular position with respect to the stator reference phase a axis,
ϕ	the angular position along the stator inner surface,
$g^{-1}(\theta_m, \Phi)$	the inverse gap function,
$N_i(\theta_m, \Phi)$	the winding function of winding *i*, and
$N_j(\theta_m, \Phi)$	the winding function of winding *j*.

The winding function of any winding represents, in effect, its MMF distribution along the air gap for a unit current in the winding. If this winding is located on the stator, the winding function is only a function of the stator periphery angle ϕ while if the winding is located on the rotor the winding must be expressed as a function of both ϕ and the mechanical position of the rotor θ_m.

The windings distributions for the two windings N_{4p} and N_{2p} can be expressed, assuming sinusoidal distribution, as:

$$N_{4p}(\phi) = N_1 \sin(2\phi) \tag{2}$$

$$N_{2p}(\phi) = N_2 \sin(\phi) \tag{3}$$

Where, N_1 and N_2 are the equivalent number of turns per phase per pole.

The inverse air gap function for the three saliencies rotor can be expressed as,

$$g^{-1}(\theta_m,\phi) = \frac{1}{g}\,,$$

$$\theta_m + \frac{\pi}{P_r}(2(n-1)-\alpha) < \phi < \theta_m + \frac{\pi}{P_r}(2(n-1)+\alpha)$$
$$= 0\,, \quad \text{otherwise} \tag{4}$$

Where,

n = 1, 2, Pr (number of saliencies),

α is the rotor pole arc to pole pitch ratio.

The windings distributions of the two windings as well as the inverse air gap function for the prototype machine are shown in fig. 2.

Substituting from eqs. (2-4) in eq. (1), different machine inductances can be calculated.

The machine self inductances of the 4-pole winding L_1 and the 2-pole winding L_2 are expressed in matrix form as,

$$L_1 = \frac{\mu_o.R.l.{N_1}^2\alpha\pi}{g} \tag{5}$$

$$L_2 = \frac{\mu_o.R.l.{N_2}^2\alpha\pi}{g} \tag{6}$$

The mutual inductances between the 4-pole and the 2-pole windings are expressed as,

$$M_{12} = -\frac{\mu_o.R.l.N_1\cdot N_2\cdot\sin(\alpha\pi)}{g}\cos(3\theta_m) \tag{7}$$

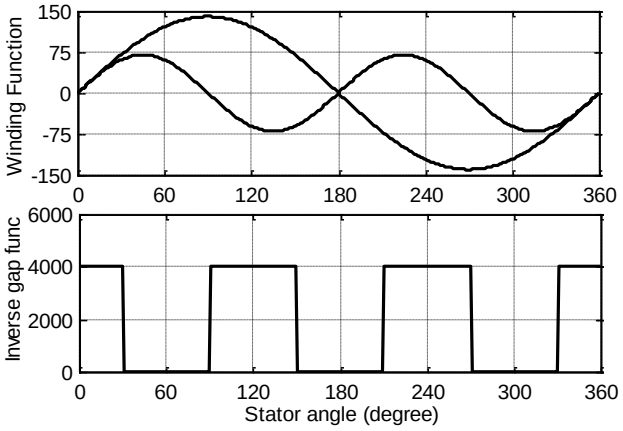

Fig. 2. Winding function for stator windings and the inverse air gap function.

Fig. 3 shows the inductance variations of the machine windings with respect to the rotor angular position. The self-inductances L_1 and

L_2 are assumed constant and independent of rotor angular position, due to the inequality of stator winding number of poles and rotor saliencies, as eqs. (5, 6) imply. The mutual inductance M_{12} varies sinusoidally with rotor angular position.

Fig. 4 illustrates the measured output voltage of the prototype model when the speed is 1000 r.p.m., at dc excitation of 1.2 A, 28V.

4. Theory of operation

When MPM is doubly fed, it operates steadily at mechanical synchronous speed given by [14]:

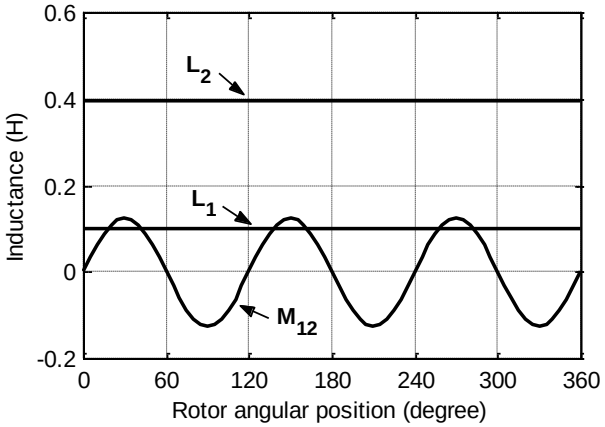

Fig. 3. Inductance variation with respect to the rotor angular position.

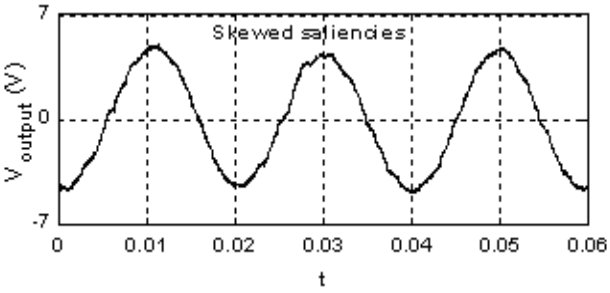

Fig. 4. Output Voltage of the tachogenerator.

$$\omega_m = \frac{\omega_1 - \omega_2}{P_r} \quad , \tag{8}$$

where ω_1, ω_2 are the frequency of the auxiliary and excitation winding respectively while ω_m is the mechanical speed in rad/sec. ω_2, has a negative sign when the two stator fields are in the same direction, while the rotor saliencies $P_r = P_1 + P_2$

The excitation winding is connected to a supply with constant frequency ω_2, while the auxiliary winding frequency ω_1 is determined according to the speed ω_m. Also, if the auxiliary winding is polyphase it is assumed to have reversed phase sequence with respect to the excitation winding.

The machine d-q equations written in the stationary reference frame are [14]:

$$\begin{aligned}
\lambda_{d1} &= L_1 i_{d1} + M_{12}\, i_{d2} \\
\lambda_{q1} &= L_1 i_{q1} - M_{12}\, i_{q2} \\
\lambda_{d2} &= M_{12}\, i_{d1} + L_2 i_{d2} \\
\lambda_{q2} &= -M_{12}\, i_{q1} + L_2 i_{q2} \ .
\end{aligned} \tag{9}$$

$$\begin{aligned}
v_{d1} &= R_1 i_{d1} + \frac{d\lambda_{d1}}{dt} \\
v_{q1} &= R_1 i_{q1} + \frac{d\lambda_{q1}}{dt} \\
v_{d2} &= R_2 i_{d2} + \frac{d\lambda_{d2}}{dt} + P_r \omega_m\, \lambda_{q2} \\
v_{q2} &= R_2 i_{q2} + \frac{d\lambda_{q2}}{dt} - P_r \omega_m\, \lambda_{d2} \ .
\end{aligned} \tag{10}$$

Since tachogenerators are normally connected to a high input impedance amplifiers, it is assumed that $i_1 = 0$, hence the voltage induced in the auxiliary winding and its frequency can be written as

$$\overline{v_1} = j\omega_1 M_{12} \overline{i_2}^{*} \tag{11}$$

$$\omega_1 = \omega_2 + P_r\, \omega_m \tag{12}$$

5. Simulation and experimental results

In this section simulation results are illustrated to investigate the flux distribution in the machine, the induced voltage waveform, and the change of output voltage from the proposed tachogenerator at different values of driving speeds.

A finite element model is developed to illustrate the flux distribution in the machine as shown in fig. 5. The flux density distribution along the rotor peripheral shown in fig. 6. reveals the effect of the four stator teeth facing each rotor pole.

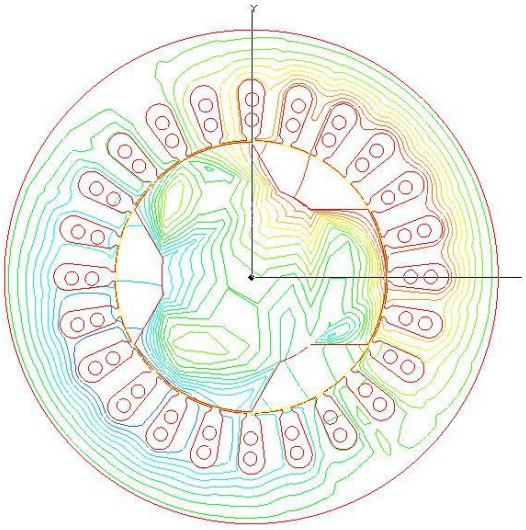

Fig. 5. Flux distribution in the tachogenerator.

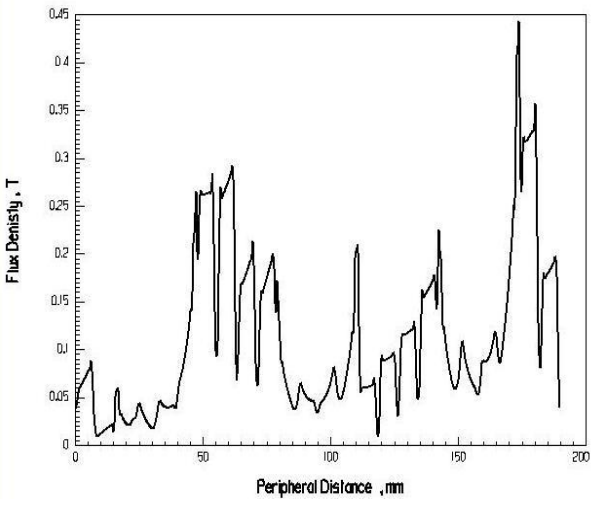

Fig. 6. Air gap flux density distribution along the peripheral distance.

For DC excitation, the 2-pole winding is connected to a dc supply. ω_2 = 0 and ω_1 is proportional to ω_m. The output voltage waveform obtained from the finite element model at 1000 rpm with dc excitation is shown in fig. 7 which matches that obtained experimentally in fig. 4.

A simulink model is developed using the systems eqs. (1-12) to illustrate the change of output voltage with linearly increasing speed for DC and AC excitations as shown in fig. 8 and fig. 9 respectively.

It is noted that, for DC excitation the output voltage is zero for zero speed. As the speed increases, the output voltage increases linearly, i.e. a linear voltage speed characteristic is obtained. Also, the output voltage frequency increases from zero according to eqs. (11-12). The low output frequency at low speeds results in ripples or delayed response when peak detector is to be used since the time interval between peaks is extended. Moreover the peak detector suffers from a voltage drop due to the diode forward voltage. This results in a blind speed range near zero speed when the output voltage is less than the diode forward voltage. This range can be minimized by increasing the gain via increasing the excitation level. However, this is limited by the excitation winding rating.

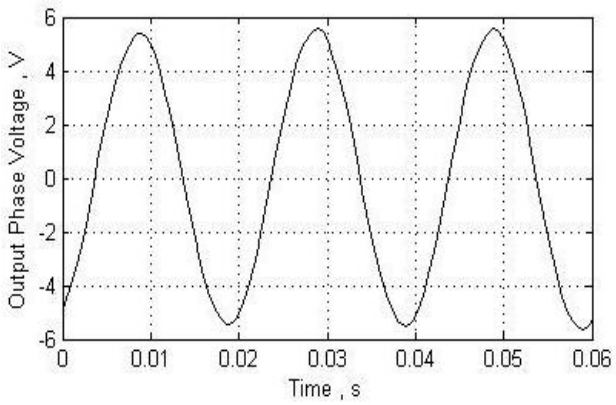

Fig. 7. Output voltage waveform.

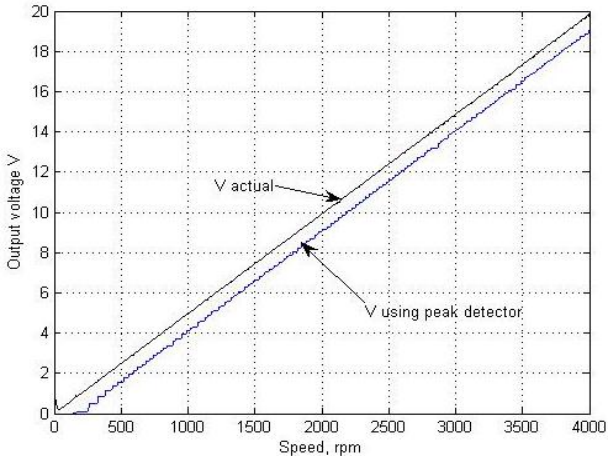

Fig. 8. Relation between speed and output voltage for DC excitation.

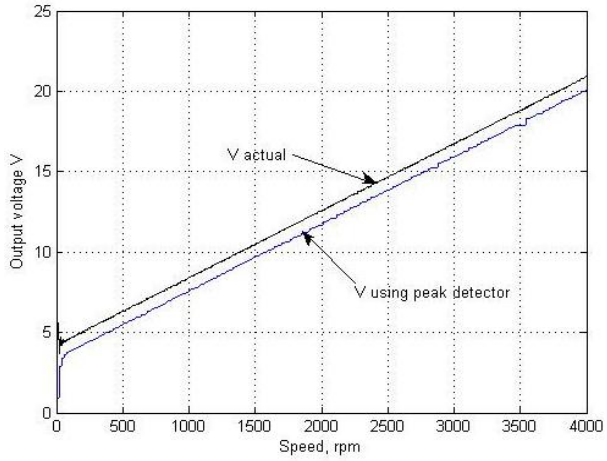

Fig. 9. Relation between speed and output voltage for AC excitation.

For AC excitation, the frequency of the voltage induced in the auxiliary winding is equal to the excitation frequency at zero speed as eq. (12) implies. This results in a smoother characteristic; compared to the DC excitation; when peak detector is to be used. Fig. 9 shows that the AC excitation has a linear voltage speed characteristic. Moreover, it has an offset value due to the transformer voltage at zero speed as expected from eq. (11). This offset mitigates the effect of diode forward voltage drop when peak detector is to be used and enable the system to provide signal at speeds near zero speed which makes AC excitation scheme to be proposed for measuring transient variations of speed.

To investigate the dynamic performance of the tachogenerator, the start up response for an induction machine is to be investigated using simulink model for the proposed tachogenerator. Figs. 10 and 11 illustrate the change of output voltage with time during starting up for DC and AC excitations. For DC excitation, the output of the peak detector suffers from a blind period due to the diode forward voltage drop and the low frequency of the voltage near zero speed. Although the actual voltage increases gradually, the low frequency of the output voltage at low speeds appears as steps when peak detector is to be used. This makes peak detector not suitable for low speeds, when DC excitation is to be used, and more complicated techniques are to be used to measure the output voltage. As the speed increases, the output voltage increases and characteristic becomes smooth. When AC excitation is used, the frequency of the output voltage is the same frequency of the excitation voltage at zero speed as indicated by eq. (12). Fig. 11 shows that when AC excitation is used, there is no blind period and simple peak detector can be used to provide a smoother linear voltage / speed characteristic.

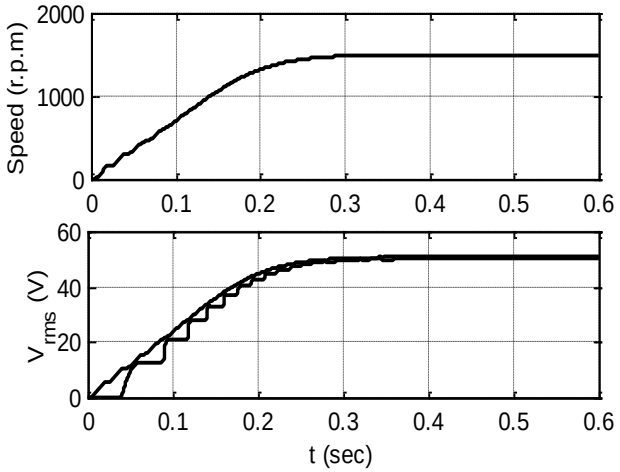

Fig. 10. The tachogenerator actual and peak detector output voltage with DC excitation during induction motor start up.

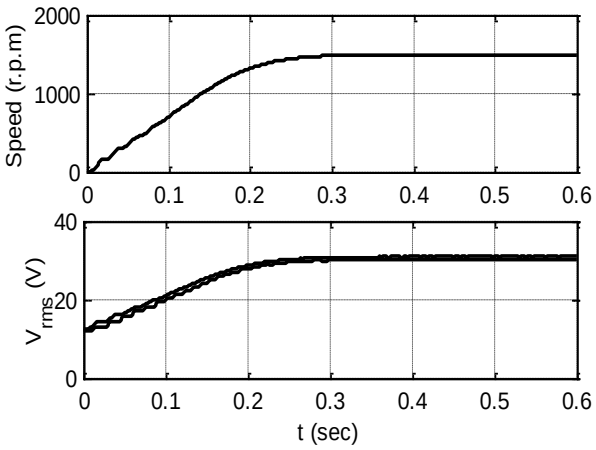

Fig. 11. The tachogenerator actual and peak detector output voltage with AC excitation during induction motor start up.

6. Conclusions

This paper presents a new application for the Reluctance type Mixed Pole Machine (MPM) as a tachogenerator. Expressions for the machine inductances were given using winding function method. A finite element and dynamic model based on the system equations were developed to illustrate the flux distribution in the machine and the induced voltage waveforms and to obtain the voltage speed relationship for DC and AC excitation. The proposed tacho is a simple in construction brushless machine. It has salient rotor with no rotor winding, which results in an inertia lower than that of the commonly used induction tachogenerators. The proposed system shows a linear voltage / speed relationship over a wide speed range. These merits make the proposed system competitive in the speed measuring area.

Nomenclature

v_{d1},v_{q1}, v_{d2}, v_{q2}	2-axis machine voltages,
i_{d1}, i_{q1}, i_{d2}, i_{q2}	2-axis machine currents,
λ	Flux linkage,
L_1, L_2, M_{12}	Machine inductances per phase,
R_1, R_2	Machine resistance per phase,
f_1, ω_1	Stator (1) frequency,
f_2, ω_2	Stator (2) frequency,
P_1	No of pole-pairs of Stator (1),
P_2	No of pole-pairs of Stator (2),
P_r	No of rotor saliencies,
ω_m	Rotor mechanical speed rad/s,
R	Rotor radius,
l	Rotor length,
μ_o	Space Permeability
θ_m	The rotor angular position with respect to the stator reference phase a axis, and
ϕ	Angular position along the stator inner surface.

Suffices

d, q	*d-q* (synchronous) axes
1, 2	Stator (1), stator (2)

Appendix

MPM machine data

Rated Power	250 Watt
Rated 4-pole voltage	60 V
Rated 4-pole current	2.1 A
Rated 4-pole frequency	50 Hz
Control 2-pole voltage	0 to 120 V
Rated 2-pole current	1.2 A
Control 2-pole frequency	-50 to 50 Hz

Number of turns per phase per pole

2-pole winding	140 turn
4-pole winding	70 turn
Machine Dimensions	
Rotor radius	3 cm
Rotor length	8.5 cm
Air gap length	0.375 mm

Machine Parameters

4-pole stator:
R_1 = 22.3 Ω, L_1 = 0.1084 H
2-pole stator:
R_2 = 23.43 Ω, L_2 = 0.4072 H
Mutual Inductance between two stators:
M_{12} = 0.115 H

References

[1] A.E. Corbett, "An Axial Airgap Brushless DC Tachogenerator", IEE Colloquium on Instrumentation of Rotating Electrical

Machines, London, 12 Feb., pp. 3/1 - 3/3 (1991).
[2] O.A. Turcanu and V. Fireteanu, "Field-Circuit-Motion Numerical Models of the AC Tachogenerator with Rotor of Solid Conductor Type", IEEE International Electric Machines and Drives Conference, 2007, IEMDC '07, Antalya, 3-5 May, Vol. 2, pp. 1102 – 1107 (2007).
[3] A.R.W. Broadway and L. Burbridge, "Self-Cascaded Machine: A Low-Speed Motor or High-Frequency Brushless Alternator", IEE Proc., Vol. 117 (7), July, pp. 1277-1290 (1970).
[4] A.R. Munoz and T.A. Lipo, "Dual Stator Winding Induction Machine Drive", IEEE Trans. on Industry Applications, Vol. 36 (5), September/October, pp. 1369–1379 (2000).
[5] O. Ojo and W. Zhiqiao, "Modeling of a Dual-Stator-Winding Induction Machine Including the Effect of Main Flux Linkage Magnetic Saturation", IEEE Trans. on Industry Applications, Vol. 44 (4), July/August, pp. 1099–1107 (2008).
[6] O. Ojo and W. Zhiqiao, "Speed Control of a Dual Stator Winding Induction Machine", 22nd Annual IEEE Applied Power Electronics Conference, APEC 2007 – February/March, pp. 229–235 (2007).
[7] E. Spooner and A.C. Williamson, "Mixed Pole Windings and Some Applications", IEE Proc. B, Electric Power Applications, Vol. 137 (2), March, pp. 89–97 (1990).
[8] R.E. Betz and M.G. Jovanovic, "Theoretical Analysis of Control Properties for the Brushless Doubly Fed Reluctance Machine", IEEE Trans. on Energy Conversion, Vol. 17 (3), Sept., pp. 332–339 (2002).
[9] M.G. Jovanovic, Y. Jian and E. Levi, "Encoderless Direct Torque Controller for Limited Speed Range Applications of Brushless Doubly Fed Reluctance Motors", IEEE Trans. Industry Applications, May-June, Vol. 42 (3), pp. 712–722 (2006).
[10] E.M. Schulz and R.E. Betz, "Optimal Rotor Design for Brushless Doubly Fed Reluctance Machines", Industry Application Conference, 38th Annual meeting, October, Vol. 1, pp. 256-261 (2003).
[11] A.L. Mohamadein, M.M. Ahmed and M.M. El-Daba, "Mixed-Pole Reluctance Machine with Ring-Coils on Rotor Poles (A Novel Rotor Version)", IEEE International Electric Machines and Drives Conference, IEMDC, pp. 705 – 710 (2001).
[12] A.L. Mohamadein, R.A. Hamdy and A.S. Abdel-khalik, "Transient Model of Mixed Pole Machines with Eccentric Reluctance Rotor", Alexandria Engineering Journal AEJ, Vol. 43 (4), July, pp. 455-466 (2004).
[13] A.L. Mohamadein, R.A. Hamdy and A.S. Abdel-khalik, "Novel Modeling Technique that Adopts Radial Force Generated in Mixed Pole Generators", Alexandria Engineering Journal AEJ, Vol. 43 (4), July, pp. 467 – 476 (2004).
[14] A.L. Mohamadein, R.A. Hamdy and A.S. Abdel-khalik, "Performance of Mixed Pole Machines as Stand-Alone Generator", the 16th International Conference on Electrical Machines - ICEM, 5-8 Septemeber, Cracow – Poland (2004).
[15] A.L. Mohamadein, R.A. Hamdy and A.S. Abdel-khalik, "Stand Alone Self-Excited Mixed Pole Generator", EPE-PEMC 2004, European Power Electronics – Power Electronics and Machine Control, 2-4 September, Riga, Latvia, A54285 (2004).
[16] F. Valenciaga and P.F. Puleston, "Variable Structure Control of a Wind Energy Conversion System Based on a Brushless Doubly Fed Reluctance Generator", IEEE Trans. Energy Conversion, Vol. 22 (2), pp. 449–506 (2007).
[17] Y. Fan, K.T. Chau and S. Niu, "Development of a New Brushless Doubly Fed Doubly Salient Machine for Wind Power Generation", IEEE Trans. Magn., Vol. 42 (10), pp. 3455–3457 (2006).
[18] Y. Fan and T.K. Chau, "Design Modelling and Analysis of a Brushless Doubly Fed Doubly Salient Machine for Electric Vehicles", IEEE Trans. Ind. Appl., Vol. 44 (3), pp. 727–734 (2008).
[19] A.S. Abdel-Khalik, M.I. Masoud, A.L. Mohamadein, B.W. Williams and M. Magdy, "Control of Rotor Torque and

Rotor Electric Power of a Shaft-Mounted Electrical Load in a Mixed Pole Machine", Electric Power Applications, IET, Vol. 3, Issue 4, July, pp. 265 – 278 (2009).

[20] L. Xu, F. Liang and T.A. Lipo, "Transient Model of a Doubly Excited Reluctance Motor", IEEE TRANS on Energy Conversion, Vol. 6 (1), March, pp. 126-133 (1991).

[21] M.M. El-Daba, "Mixed Pole Machine" PhD Thesis, Faculty of Engineering, Alexandria University, Egypt (2001).

Received August 23, 2009
Accepted September 24, 2009